Inorganica Chimica Acta 391 (2012) 121–129

Contents lists available at SciVerse ScienceDirect

Inorganica Chimica Acta

journal homepage: www.elsevier.com/locate/ica

# Synthesis, crystal structure, DNA-binding properties, cytotoxic and antioxidation activities of several ternary copper(II) complexes with a new reduced Schiff base ligand

Lei Jia [a,*], Jie Shi [b], Zhi-hong Sun [b], Fei-fei Li [a], Yuan Wang [a], Wei-na Wu [a], Qin Wang [b,*]

[a] Department of Physics and Chemistry, Henan Polytechnic University, Jiaozuo 454000, PR China
[b] Institute of Cancer Biology and Drug Screening, School of Life Science, Lanzhou University, Lanzhou 730000, PR China

ARTICLE INFO

*Article history:*
Received 8 July 2011
Received in revised form 13 March 2012
Accepted 20 May 2012
Available online 30 May 2012

*Keywords:*
Ternary copper(II) complexes
Cytotoxicity
DNA-binding properties
Reduce Schiff base
X-ray crystallography
Phenanthroline base

ABSTRACT

Three new ternary copper(II) complexes, $[Cu_2(phen)_2(PDIMAla)(H_2O)_2](ClO_4)_2{\cdot}CH_3OH$ (**1**), $[Cu_2(dpq)_2(PDIMAla)(H_2O)_2](ClO_4)_2{\cdot}CH_3OH$ (**2**) and $[Cu_2(dppq)_2(PDIMAla)(H_2O)_2](ClO_4)_2{\cdot}CH_3OH$ (**3**) (phen = 1,10-phenanthroline, dpq = dipyrido[3,2:2′,3′-f]quinoxaline, dppz = dipyrido[3,2-a:2′,3′-c]phenazine, $H_2$PDIMAla = *N,N′-(p*-xylylene)di-alanine acid) have been synthesized and the complex **1** has been structurally characterized by single-crystal X-ray crystallography, spectrometric titrations, ethidium bromide displacement experiments, CD (circular dichroism) spectral analysis and viscosity measurements. The results indicate that the three compounds, especially the complex **3**, can strongly bind to calf-thymus DNA (CT–DNA). The intrinsic binding constants $K_b$ of the ternary copper(II) complexes with CT–DNA are $0.38 \times 10^5$, $1.4 \times 10^5$ and $7.8 \times 10^5$ for **1**, **2** and **3**, respectively. Comparative cytotoxic activities of the copper(II) complexes are also determined by acid phosphatase assay. The results show that the ternary copper(II) complexes have significant cytotoxic activity against the human hepatic (HepG2), human promyelocytic leukemia (HL60) and human prostate (PC3) cell lines. Investigation of antioxidation property show that all the copper(II) complexes have strong scavenging effects for hydroxyl radicals.



## 1. Introduction

Currently, cancer is the second cause of death, accounting for about a quarter of all deaths [1]. Nearly one half of all cancers that are diagnosed result in the death of the patient, so that the development of new anticancer therapies is one of the fundamental goals in medicinal chemistry.

It is well known that copper is an essential element in human normal metabolism. In biological systems, copper exists as a variety of complexes which due to that the coordinated forms of copper are more stable than the corresponding ionic species [2,3]. Therefore, the copper complexes of non-steroidal anti inflammatory compounds such as aspirin and niflumic acid have been studied as they show good antiarthritic activity [4]. These complexes have been found to be more active and desirable drugs than the ligands themselves, suggesting that the activity of such metal based drugs may be due to the *in vivo* formation of metallic complexes [5]. So that the synthesis and studies of metal complexes with active drugs as ligands increase the interest for inorganic, pharmaceutical and medicinal chemistry and concentrate much attention as an approach to new drug development [6].

1,10-Phenanthroline (Phen) and its substituted derivatives, both in the metal-free state and as ligands coordinated to transition metals, disturb the functioning of a wide variety of biological systems [7]. Furthermore, when metal-free *N,N′*-chelating bases are found to be bioactive, it is usually assumed that sequestering of trace metals *in situ* is involved, and that the resulting metal complexes are the active species [8–11]. One of the most biologically active of the metal–phen complexes is $[Cu(phen)_2]^{2+}$. Tsang and coworkers [12] reported that incubation of a human hepatic cell line (Hep-G2) with $[Cu(phen)_2]^{2+}$ resulted in internucleosomal DNA fragmentation. Transition metal cations, such as Cu(II) and Fe(II), can bind to negatively charged DNA and have been shown to play an important role in the local formation of $OH^{\cdot}$ radicals [13–15].

Further more, ternary complexes of Cu(II) with substituted phenanthrolines (phens) have been reported and their cytotoxic properties are evaluated recently [16–18]. The most potent complex is bis(diisopropylsalicylato)(2,9-dimethylphenanthroline)copper(II), which exhibits cytotoxicity comparable with the anticancer drug cisplatin $[PtCl_2(NH_3)_2]$ [19]. Their cytotoxicity may be due to chelation of transition metals such as copper or iron for example in the test media. These biological activities are improved by the

* Corresponding authors. Tel.: +86 391 3987818 (L. Jia), +86 931 8915350 (Q. Wang).
*E-mail addresses:* jlxj@hpu.edu.cn (L. Jia), qwang@lzu.edu.cn (Q. Wang).

0020-1693/$ - see front matter © 2012 Elsevier B.V. All rights reserved.
http://dx.doi.org/10.1016/j.ica.2012.05.014

complexation with some divalent transition metals. Thus, antiviral activity is found for divalent transition metals chelates with substituted phenanthrolines [20]. Moreover, such complexes are used as DNA intercalating agents and have been found useful for examining distinctive conformations along the DNA helix [21].

Herein we report the synthesis, crystal structure, DNA-binding, cytotoxic and antioxidation activities of a series of ternary copper(II) complexes $[Cu_2(D)_2(PDIMAla)(H_2O)_2](ClO_4)_2{\cdot}CH_3OH$ (**1**–**3**) containing D as 1,10-phenanthroline (phen, **1**), dipyrido[3,2-d:2′,3′-f]quinoxaline (dpq, **2**), dipyrido[3,2-a:2′,3′-c]phenazine (dppz, **3**) (Scheme 1). The primary aim of the current study is to determine the cancer chemotherapeutic potential of metal-free phen and its substituted derivatives by using three human-derived cancer model cell lines of human hepatic (HepG2), human promyelocytic leukemia (HL60) and human prostate (PC3). In order to illustrate that the effect observed is due to the complexes rather than the free metal ions, the anti-tumour activities of the simple Cu(II) salt is also determined. The work represents the first assessment of the potential application of the three copper(II) complexes **1**–**3** as novel therapeutic agents for the treatment of cancer.

## 2. Experimental

### 2.1. Materials and instrumentation

All starting materials were obtained commercially and used as received. Calf thymus DNA (CT–DNA) and ethidium bromide (EB) were obtained from Sigma Chemical Co. All the measurements involving the interactions of the three metal complexes with CT–DNA were carried out in doubly distilled water buffer containing 5 mM Tris and 50 mM NaCl, and adjusted to pH 7.1 with hydrochloric acid. UV–Vis spectrometer was employed to check the solution of CT–DNA purity ($A_{260}$: $A_{280} > 1.80$) and the concentration ($\varepsilon = 6600\ M^{-1}\ cm^{-1}$ at 260 nm) in the buffer. The ternary copper(II) complexes were dissolved in a mixture solvent of 5% $CH_3OH$ and 95% Tris–HCl buffer (5 mM Tris–HCl, 50 mM NaCl, pH 7.1) at concentration $1 \times 10^{-3}$ M.

The UV–Vis absorption spectra were recorded using a Varian Cary 100 spectrophotometer and fluorescence emission spectra were recorded using a Hitachi F-4500 spectrofluorophotometer. The elemental analyses were performed in the microanalytical laboratory, Department of Chemistry, National University of Singapore. The $^1H$ NMR spectra was recorded with a Bruker ACF300 FT-NMR instrument using TMS as an internal reference in $D_2O$ for the ligand. The infrared spectra (KBr pellet) were recorded using an FTS165 Bio-Rad FTIR spectrophotometer in the range of 4000–400 $cm^{-1}$. ESI mass spectra were recorded on a Finnigan MAT LCQ mass spectrometer using the syringe pump method. The CD spectra were recorded on a Jasco J-810 spectropolarimeter. The antioxidant activites were tested on a 721E spectrophotometer (Shanghai Analytical Instrument Factory, China).

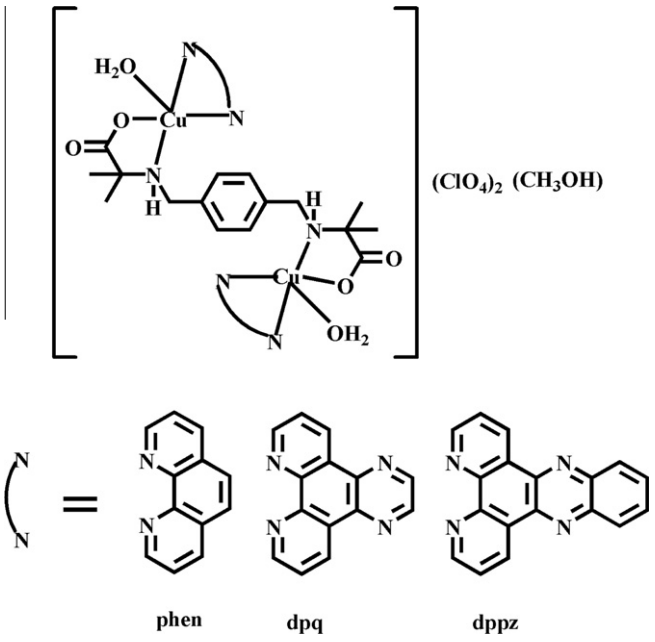


**Scheme 1.** Complexes **1**–**3** and the heterocyclic bases.

### 2.2. Synthesis of the ligand ($H_2PDIMAla$)

$H_2PDIMAla$: *N,N′-(p*-xylylene)di-(2-methyl) alanine acid. To a solution of 2-amino-2-methyl propanoic acid (1.03 g, 10 mmol) and NaOH (0.4 g, 10 mmol) in 20 mL of MeOH and 10 mL of water was added terephthalaldehyde (0.67 g, 5 mmol) in 20 mL of MeOH. The yellow solution was stirred for 3 h at room temperature prior to cooling in an ice bath. The intermediate Schiff base that formed was reduced with an excess of $NaBH_4$ (0.46 g, 12 mmol) in MeOH containing a few drops of NaOH solution. The yellowish color was slowly discharged, after stirring for another 1 h, the solution was acidified with acetic acid to a pH of 5.0–6.0. The resulting colorless solid was filtered off, washed with dry MeOH and $Et_2O$, and recrystallized from $H_2O$/EtOH (1:3) after drying in air. Yield: 1.37 g (89%). *Anal.* Calc. for $C_{16}H_{24}N_2O_4$: C, 62.32; H, 7.84; N, 9.08. Found: C, 62.51; H, 7.63; N, 9.26%. ESI–MS Calc. for $C_{14}H_{20}N_2O_4$: 308.37. Found: 307.3%. $^1H$ NMR ($D_2O$) $\delta$ 1.38 (s, 12H), 3.85 (s, 4H), 7.42 (d, 4H). IR (KBr, $cm^{-1}$): $\nu$(NH) 3071, $\nu(CH_2)$ 2986, $\nu(COO^-)$ 1612, 1354.

### 2.3. Synthesis of the complex $[Cu_2(phen)_2(PDIMAla)(H_2O)_2](ClO_4)_2{\cdot}CH_3OH$ (**1**)

To the green solution formed from $Cu(ClO_4)_2{\cdot}6H_2O$ (0.371 g, 1 mmol) in MeOH (8 mL) and phen (0.181 g, 1 mmol) in MeOH (8 mL) was added a filtered solution of $H_2PDIMAla$ (0.154 g, 0.5 mmol) in $H_2O$ (20 mL) containing LiOH. The resulting blue solution was stirred for 1 h and then filtered and left for a week, after which time the blue crystals were isolated by filtration. Yield: 0.651 g, 92 %. *Anal.* Calc. for $C_{41}H_{46}Cl_2Cu_2N_6O_{15}$: C, 46.62; H, 4.37; N, 7.92. Found: C, 46.81; H, 4.56; N, 8.17%. IR (KBr, $cm^{-1}$): $\nu$(NH) 2987, $\nu(CH_2)$ 2927, $\nu(COO^-)$ 1595, 1386. $\nu$(Cl-O) 1089.

### 2.4. Synthesis of the complex $[Cu_2(dpq)_2(PDIMAla)(H_2O)_2](ClO_4)_2{\cdot}CH_3OH$ (**2**)

To the green solution formed from $Cu(ClO_4)_2{\cdot}6H_2O$ (0.371 g, 1 mmol) in MeOH (8 mL) and dpq (0.232 g, 1 mmol) in MeOH (8 mL) was added a filtered solution of $H_2PDIMAla$ (0.154 g, 0.5 mmol) in $H_2O$ (20 mL) containing LiOH. The resulting blue solution was stirred for 6 h, the blue precipitate were isolated by filtration. Yield: 0.469 g, 62%. *Anal.* Calc. for $C_{45}H_{46}Cl_2Cu_2N_{10}O_{15}$: C, 46.40; H, 3.98; N, 12.02. Found: C, 46.31; H, 4.01; N, 12.31%. IR (KBr, $cm^{-1}$): $\nu$(NH) 2973, $\nu(CH_2)$ 2912, $\nu(COO^-)$ 1631, 1388. $\nu$(Cl-O) 1083.

### 2.5. Synthesis of the complex $[Cu_2(dppz)_2(PDIMAla)(H_2O)_2](ClO_4)_2CH_3OH$ (**3**)

To the green solution formed from $Cu(ClO_4)_2{\cdot}6H_2O$ (0.371 g, 1 mmol) in MeOH (8 mL) and dpz (0.282 g, 1 mmol) in MeOH (8 mL) was added a filtered solution of $H_2PDIMAla$ (0.154 g, 0.5 mmol) in $H_2O$ (20 mL) containing LiOH. The resulting blue

solution was stirred for 6 h, the blue precipitate were isolated by filtration. Yield: 0.532 g, 66%. *Anal.* Calc. for $C_{53}H_{50}Cl_2Cu_2N_{10}O_{15}$: C, 50.32; H, 3.98; N, 11.07. Found: C, 50.55; H, 4.32; N, 11.29%. IR (KBr, $cm^{-1}$): $\nu$(NH) 3094, $\nu(CH_2)$ 2920, $\nu(COO^-)$ 1636, 1357. $\nu$(Cl-O) 1080.

*Caution.* Perchlorate salts of metal complexes containing organic ligands are potentially explosive. Only small quantity of material should be prepared and handled with suitable safety measures.

### 2.6. X-ray crystallography

Details of the crystal parameters, data collection and refinements of complex **1** were listed in Table 1. Selected bond lengths and bond angles were listed in Table 2. Main intra and intermolecular hydrogen bonds were listed in Table 3. Single crystal X-ray diffraction measurements were made on a Bruker AXS SMART CCD diffractometer with Mo Kα ($\lambda$ = 0.71073 Å) in a sealed tube. Unit cell dimensions were obtained with least-squares refinements, and all structures were solved by direct methods. The program SMART[41] was used to collect the intensity data, SAINT [22] for integration of the intensity [22], SADABS [23] for absorption correction and SHELXTL [24] for structure solution and refinements on $F^2$. All non-H atoms were located from successive Fourier maps, and hydrogen atoms were refined using a riding model. Anisotropic thermal parameters were used for all non-H atoms, and fixed isotropic parameters were used for H atoms. H atoms attached to N and O were located from difference Fourier maps and refined with N–H distances fixed at 0.85 (2) Å ($U_{iso}$(H) = 1.2 $U_{eq}$(N)) and O–H distances fixed at 0.85 (2) Å ($U_{iso}$(H) = 1.2 $U_{eq}$(O)). The asymmetric unit contains one half of the dinuclear molecule and the symmetry operation relates the two halves is $1-x$, $-y$, $-z$. Three oxygen atoms of the perchloride anion was disordered into two positions with occupancy ratio 56:44.

### 2.7. Spectroscopic studies on DNA interaction

#### 2.7.1. Electronic absorption spectra

Electronic absorption titration of the ternary copper(II) complex samples in the aqueous buffer solution (50 mM NaCl-5 mM Tris–HCl, pH 7.1) were performed at a fixed complex concentration (10 μM) while gradually increasing the concentration of CT–DNA. The absorption data were analyzed to evaluate the intrinsic binding constant $K_b$, which can be determined from Eq. (1) [25],

**Table 1**
Selected crystallographic data for **1**.

| Compound | **1** |
|---|---|
| Empirical formula | $C_{41}H_{46}Cl_2Cu_2N_6O_{15}$ |
| Formula weight | 1060.82 |
| Temperature (K) | 223(2) |
| Crystal system Triclinic | Monoclinic |
| Space group | *P*2(1)/c |
| *a* (Å) | 10.5259(6) |
| *b* (Å) | 18.6643(10) |
| *c* (Å) | 11.6372(7) |
| α (°) | 90 |
| *β* (°) | 95.7630(10)° |
| *γ* (°) | 90 |
| Volume ($Å^3$) | 2274.7(2) |
| *Z* | 2 |
| Calculated density ($Mg/m^3$) | 1.549 |
| Absorption coefficient ($mm^{-1}$) | 1.127 |
| Number of parameters/restraints | 340/76 |
| Measured reflections | 15,394 |
| Independent reflections | 5231 |
| Final R indices [$I > 2\sigma(I)$] | 0.0491, 0.1330 |
| Goodness-of-fit on $F^2$ | 1.042 |
| Largest difference peak and hole (e $Å^{-3}$) | 0.623 and −0.423 |

**Table 2**
Selected bond lengths (Å) and bond angles (°) for complex **1**.

| | | | |
|---|---|---|---|
| Cu(1)–O(1) | 1.928(2) | Cu(1)–N(2) | 1.998(2) |
| Cu(1)–N(3) | 2.012(2) | Cu(1)–N(1) | 2.033 (2) |
| Cu(1)–O(1W) | 2.272(3) | | |
| O(1)–Cu(1)–N(2) | 178.50(9) | O(1)–Cu(1)–N(3) | 82.58(9) |
| N(2)–Cu(1)–N(3) | 98.51(9) | O(1)–Cu(1)–N(1) | 95.75(10) |
| N(2)–Cu(1)–N(1) | 82.76(10) | N(3)–Cu(1)–N(1) | 143.83(9) |
| O(1)–Cu(1)–O(1W) | 87.15(11) | N(2)–Cu(1)–O(1W) | 93.13(11) |

**Table 3**
Main intra and intermolecular hydrogen bonds for the complex **1** (Å, °).

| D–H···A | *d*(D–H) | *d*(H···A) | *d*(D···A) | <(DHA) |
|---|---|---|---|---|
| O1w–H1w···O5 | 0.85(2) | 2.22(5) | 2.933(10) | 178(5) |
| O1w–H2w···O6 | 0.85(2) | 2.16(4) | 2.906(5) | 173(4) |
| N3–H3N···O2 | 0.85(2) | 2.03(3) | 2.783(3) | 163(3) |

$$[DNA]/(\varepsilon_b - \varepsilon_f) = [DNA]/(\varepsilon_b - \varepsilon_f) + 1/K_b(\varepsilon_b - \varepsilon_f) \quad (1)$$

where [DNA] is the concentration of DNA in base pairs, the apparent absorption coefficient $\varepsilon_a$, $\varepsilon_f$ and $\varepsilon_b$ correspond to $A_{obsd}$/[M], the extinction coefficient of the free compound and the extinction coefficient of the compound when fully bound to DNA, respectively. In plots of [DNA]/($\varepsilon_a$–$\varepsilon_f$) versus [DNA], $K_b$ is given by the ratio of slope to the intercept.

#### 2.7.2. Fluorescence spectra

Further support for the ternary copper(II) complexes binding to DNA is given through the emission quenching experiment. EB is a common fluorescent probe for DNA structure and has been employed in examinations of the mode and process of metal complex binding to DNA. A 2 mL solution of 15 μM DNA and 1.5 μM EB (at saturating binding levels) was titrated by 0–80 μM ternary copper(II) complexes and the ligand ($k_{ex}$ = 500 nm, $k_{em}$ = 520.0–650.0 nm). According to the classical Stern–Volmer Eq. (2) [26]:

$$F_0/F = K_q[Q] + 1 \quad (2)$$

where $F_0$ is the emission intensity in the absence of quencher, $F$ is the emission intensity in the presence of quencher, $K_q$ is the

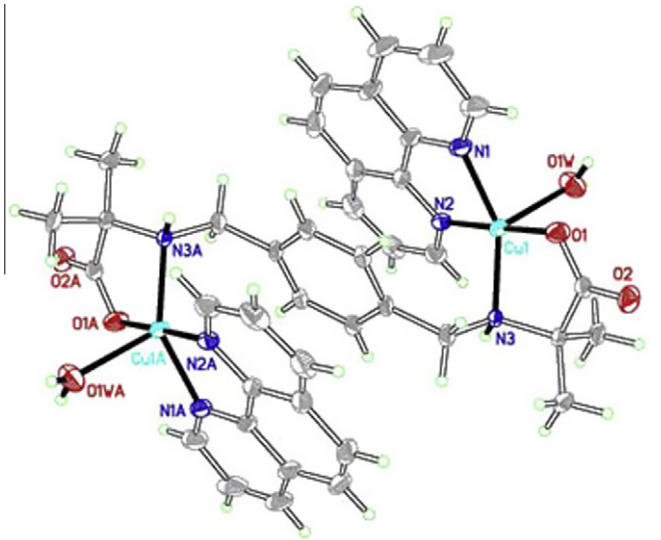


**Fig. 1.** ORTEP view of the cation in complex **1** showing 30% probability thermal ellipsoids.

quenching constant, and [Q] is the quencher concentration. The shape of Stern–Volmer plots can be used to characterize the quenching as being predominantly dynamic or static. Plots of $F_0/F$ versus [Q] appear to be linear and $K_q$ depends on temperature.

*2.7.3. Circular dichroic spectral studies*

The CD spectra of CT–DNA were recorded on a Jasco J-810 spectropolarimeter at 25 °C. The concentration of CT–DNA and the complexes were 120 and 60 μM. Each sample solution was scanned in the range of 220–370 nm. CD spectrum was generated which represented the average of three scans from which the buffer background had been subtracted.

*2.8. Viscosity measurements*

Viscosity experiments were carried out on an Ubbelodhe viscometer, immersed in a thermostated water-bath maintained to 25 °C. Titrations were performed for the ternary copper complexes (1–5 μM), and each complex was introduced into DNA solution (50 μM) present in the viscometer. Flow time was measured with a digital stopwatch and each sample was measured three times and an average flow time was calculated. Data were presented as $(\eta/\eta_0)^{1/3}$ versus the ratio of the concentration of the complex and DNA, where $\eta$ is the viscosity of DNA in the presence of complex, and $\eta_0$ is the viscosity of DNA alone. Viscosity values were calculated from the observed flow time of DNA-containing solution corrected from the flow time of buffer alone ($t_0$), $\eta = t - t_0$ [27,28].

*2.9. Cytotoxicity assay*

The reagent, *p*-nitrophenyl phosphate (*p*-NPP), was obtained from Amresco. The compounds synthesized were dissolved in dimethyl sulphoxide and diluted in culture medium. The final concentration of DMSO in cultures was always not exceeding 0.5% (v/v), which did not cause toxicity. Human hepatic (HepG2) and human prostate (PC3) cell lines were maintained in DMEM medium, human promyelocytic leukemia (HL60) were maintained in RPMI 1640 medium. Cells were cultured at 37 °C in a humidified atmosphere of 5% $CO_2$ in air. All media were supplemented with 10% fetal bovine serum and contained penicillin G (100 U/mL) and streptomycin (100 μg/mL). After the cells were seeded in 96-well plates at 4000 cells per well 12 h, they were exposed to all the tested complexes with different concentrations for 72 h. The morphological examination was performed with a Nikon ECLIPSE Ti and phase contrast images were obtained by Nikon Digital Sightds Fi1 (Nikon Corporation). The medium was removed and the wells were washed with 200 μL PBS per well. For HL-60 cells, after removing the medium and PBS, the plates were centrifuged at 2500 rpm for 10 min. One hundred microliter buffer containing 0.1 M sodium acetate (pH 5.0), 0.1% Triton X-100, and 5 mM *p*-nitrophenyl phosphate was added to each well, and then the plates were incubated for 1.5 h at 37 °C. After the reactions were stopped by adding 1 M NaOH, the absorbance was read at 405 nm by Victor$^3$ (PerkinElmer). Experiments were conducted in triplicate (three independent experiments).

*2.10. Antioxidant measurements*

The hydroxyl radicals in aqueous media were generated through the Fenton-type reaction [29,30]. The 5 mL reaction mixtures contained 2.0 mL of 100 mmol phosphate buffer (pH = 7.4), 1.0 mL of 0.10 mol aqueous safranin, 1 mL of 1.0 mmol aqueous EDTA–Fe(II), 1 mL of 3% aqueous $H_2O_2$, and a series of quantitatively microadding solutions of the tested compounds. The sample without the tested compounds was used as the control. The reaction mixtures were incubated at 37 °C for 60 min in a water-bath. Absorbance at 520 nm was measured and the solvent effect was corrected throughout. The scavenging effect for $OH^{\cdot}$ was calculated from the following expression (3) [31]:

$$\text{Suppression ratio } (\%) = [(A_i - A_0)/(A_c - A_0)] \times 100 \quad (3)$$

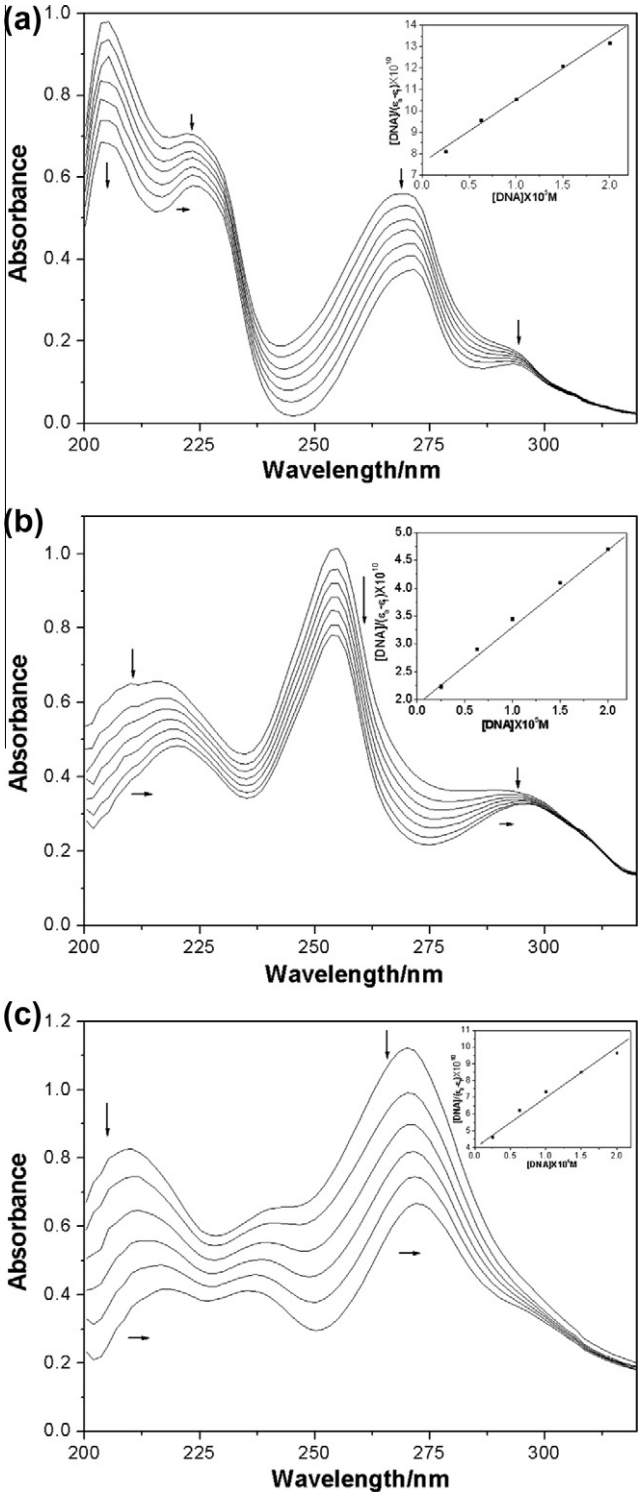


**Fig. 2.** Electronic spectra of the complex **1** (a), complex **2** (b), complex **3** (c) in Tris–HCl buffer upon addition of calf–thymus DNA. [Compound] = 10 μM, [DNA] = 0–20 μM. Arrow shows the absorbance changes upon increasing DNA concentration. Inset: plots of $[DNA]/(\varepsilon_a - \varepsilon_f)$ versus [DNA] for the titration of complex **1**–**3** with CT–DNA.

where $A_i$ is the absorbance of the sample in the presence of the tested compound, $A_0$ is the absorbance of the blank in the absence of the tested compounds and $A_c$ is the absorbance in the absence of the tested compounds and EDTA–Fe(II).

## 3. Results and discussion

### 3.1. Synthesis and general properties

Ternary copper(II) complexes containing heterocyclic bases are prepared in high yield from reactions of the reduce Schiff base ligand $H_2$PDIMAla in the presence of LiOH with copper(II) perchlorate and *N*,*N*-donor heterocyclic bases. The complexes have been characterized by elemental analysis and spectroscopic data. The stability of copper(II) complexes in an aqueous solution have been studied by observing the UV–Vis spectrums and estimating the molar conductivities at different time intervals for any possible change. The tested copper(II) complexes are prepared in DMSO solution and for experiments freshly diluted in phosphate buffer system (at pH 7.4, 7.8). Then, the UV–Vis spectrums and molar conductivities are researched at different time intervals. The investigations reveal that the UV–Vis spectra have remained unaltered for the solutions and the molar conductance values have no obvious change for very freshly prepared and for over the whole experiment (72 h). It indicates that the copper(II) complexes are quite stable in solution. The characteristic bands of the carboxylate groups are observed in the range 1595–1640 $cm^{-1}$ for asymmetric stretching and 1320–1390 $cm^{-1}$ for symmetric stretching, respectively [32]. The difference between $_{as}(COO^-)$and the $_{sym}(COO^-)$ stretching frequencies in complexes is 200 $cm^{-1}$, thus suggesting a terminal coordination mode for the carboxylate group [33]. Weak absorptions observed in the range of 2930–2990 $cm^{-1}$ can be attributed to the $_{CH2}$ of the reduce Schiff base ligand and the vibration observed in the range of 2970–3120 $cm^{-1}$ can be attributed to the $_{NH}$ of the ligand. The broad bands at 3430 $cm^{-1}$ are ascribed to the vibration of the O–H stretching of the water ligands. Two topical bands in the region near 830 and 720 $cm^{-1}$ are assigned to (C=N) of heterocyclic bases. And the topical bands in the region near 1090 $cm^{-1}$ are assigned to (Cl–O) of anion. The conductivity measurements indicate 1:2 electrolytic nature of the complexes.

### 3.2. Structure of the ternary copper complexes

The molecular structure of complex $[Cu_2(phen)_2(PDIMAla)(H_2O)_2](ClO_4)_2{\cdot}CH3OH$ (**1**) consists of dinuclear complex cations as shown in Fig. 1. Each of the $Cu^{2+}$ ions in the dimeric complex with $N_3O_2$ donor set has a distorted square pyramidal geometry. The four basal positions are occupied by two N atoms of the phen ligand, and the amine N atom and the carboxylate O atom of the ligand. The coordination sphere at the apical position is completed by O atom of the aqua ligand. The phenyl ring of the PDIMAla ligand is sandwiched between the phen ligands through – interactions, and thus the PDIMAla ligand is "S" shaped. The bond lengths of Cu(1)–O(1) (1.928(2) Å) and Cu(1)–N(3) (2.012(2) Å) are similar to those found in $Cu(L\text{-}Thr)_2{\cdot}H_2O$, where the mean Cu–O and Cu–N (O and N atoms of L-threonine) distances are 1.95(1) and 1.98(1) Å, respectively [34]. The Cu–N(phen) bond lengths of 1.998(2) and 2.033(2) Å and the bite angle N(1)–Cu(1)–N(2) of 82.76° are close to the corresponding values for some copper–phenanthroline complexes reported [35,36]. The closest distances, 3.331 and 3.666 Å are between the centre of the phenyl ring and the middle of the carbon atoms next to the nitrogen atoms of the phen ligand. The interplanar angle between the planes is 4.42°. The Cu···Cu distance in the cation, 7.819 Å, is longer than the intermolecular distance, 6.920 Å. The N–H···O hydrogen bondings between aqua ligand and carbonyl oxygen of the PDIMAla ligand along *a*-axis produce a layer structure. The $ClO_4^-$ anions, lattice water molecules are found between the grooves and cavities with the layers. The interlayers are essentially

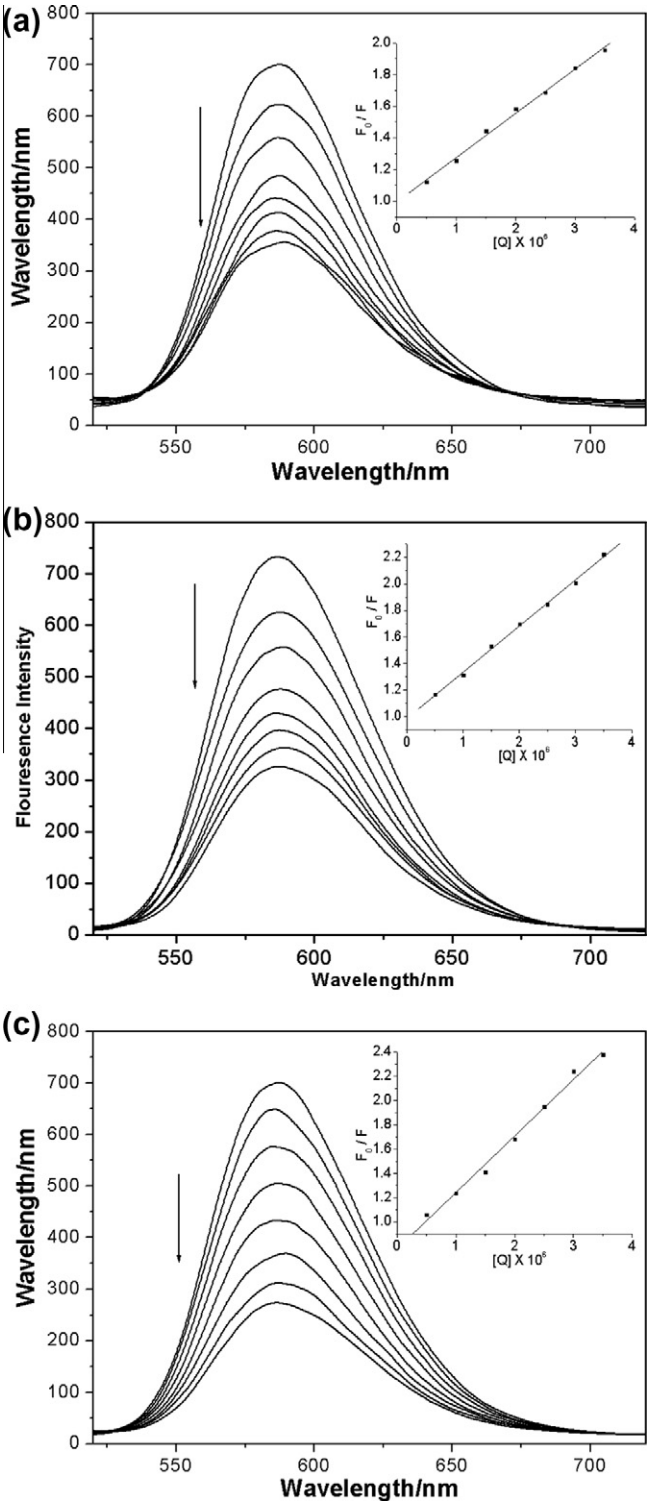


**Fig. 3.** The emission spectra of DNA–EB system (15 μM and 1.5 μM EB), $_{ex}$ = 500 nm, $_{em}$ = 520–720 nm, in the presence of the complex **1** (a), complex **2** (b), complex **3** (c). [DNA] = 10 μM, [Compound] = 0–35 μM. Arrow shows the emission intensity changes upon increasing complex concentration. Inset: Stern–Volmer plot of the fluorescence titration data of the complexes **1**–**3**.

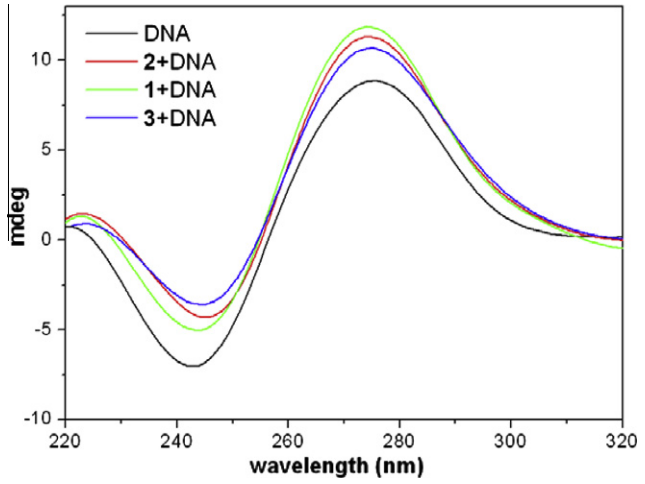


**Fig. 4.** CD spectra of CT–DNA (120 μM) in the absence and presence of the copper(II) complexes **1**, **2** and **3** (60 μM).

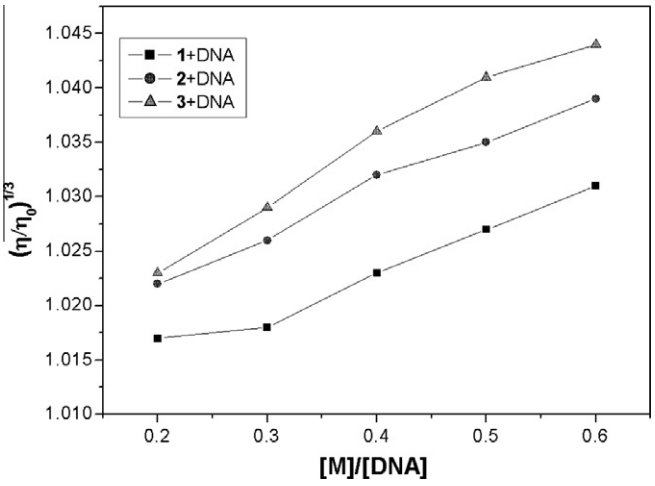


**Fig. 5.** Effect of increasing amounts of complexes **1**, **2** and **3** on the relative viscosity of CT–DNA at 25.0 °C.

held by ··· interactions as the complex **1** shows chemically significant face to face ··· aromatic stacking inter-planar distance of 3.357 Å.

### 3.3. Interactions with CT-DNA

#### 3.3.1. Electronic absorption spectra

The interactions of metal complexes with DNA have been the subject of interest for the development of effective chemotherapeutic agents. Transition metal centers are particularly attractive moieties for such research since they exhibit well-defined coordination geometries and also often possess distinctive electrochemical or photophysical properties, thus enhancing the functionality of the binding agent [37].

In the UV region of the electronic spectra, the absorption bands around 300 nm observed can be attributed to the –* transition of the coordinated ligands, while the intense electronic bands observed in the spectral range 600–700 nm are assignable to the *d–d* band, which is in agreement with five-coordinate geometry. The binding of ternary copper(II) complexes to DNA helix have been characterized through absorption spectral titrations, by following changes in absorbance and shift in wavelength. Fig. 2 shows the absorption spectra of ternary copper(II) complexes in the absence and presence of CT–DNA. Addition of increasing amounts of CT–DNA result in hypochromism and red shift. With increasing DNA concentration, the absorption bands of the three complexes show decreases in molar absorptivity (hypochromism) as well as slight bathochromism. The observed red-shift is an evidence of the stabilization of the CT DNA duplex and the hypochromism may be attributed to interaction between the aromatic rings of the complexes and DNA base pairs [38].

**Table 4**
The anti-cancer activity of the free ligand, free metal salt and complexes **1**–**3** against human hepatic cell line (HepG2), human promyelocytic leukemia cell line (HL60) and human prostate cancer cell line (PC3) expressed as $IC_{50}$ (μM).

| Test compound | Toxicities ($IC_{50}$) | | |
|---|---|---|---|
| | HepG2 | HL60 | PC3 |
| $Cu(ClO_4)_2 6H_2O$ | >160 | >160 | >160 |
| $H_2$PDIMAla | >160 | >160 | >160 |
| phen | 4.1 | 6.2 | >160 |
| dpz | 40 | 10 | >160 |
| dppz | 85 | 50 | >160 |
| **1** | 2.2 | 2.7 | 2.4 |
| **2** | 2.7 | 2.2 | 2.7 |
| **3** | 1.4 | 1.5 | 1.4 |

The $K_b$ values of ternary copper(II) complexes with different numbers of copper chelates are $0.38 \times 10^5$, $1.4 \times 10^5$, and $7.8 \times 10^5$ for **1**, **2** and **3**, respectively, the significant difference in DNA binding affinity of the three ternary copper(II) complexes can be understood as a result of the fact that the extended planar structure of the dpq and dppz ligands greatly facilitating non-covalent interactions with the DNA molecule. Compounds binding to DNA through intercalation usually results in hypochromism and bathochromism due to intercalative mode involving a strong stacking interaction between an aromatic rings and DNA base pairs [39]. All these results suggest that metal complexes can interact with CT DNA quite probably by intercalating the compounds into DNA base pairs [40].

It is noteworthy that the $K_b$ values are higher than the binding affinity of EB for DNA, ($K_b$ = 1.23 (±0.07) × $10^5$ $M^{-1}$) [41], suggesting that the existing interactions may cause EB displacement from its complex with DNA [41]. Interestingly, the $K_b$ values obtained for the above ternary copper(II) complexes are higher than those for the other known mononuclear and binuclear copper(II) complexes containing 1,10-phenanthroline ([Cu(phen)(L-Thr)($H_2O$)]($ClO_4$) ($K_b$, $6.35 \times 10^3$ $M^{-1}$) [11], [$Cu_2$(phen)$_2Cl_4$] ($K_b$, $4.75 \times 10^4$ $M^{-1}$) [42], [(phen)Cu(bipp)Cu(phen)]($ClO_4$)$_4$ ($K_b$, $1.4 \times 10^4$ $M^{-1}$) [43]. This showed that comparatively the ternary copper(II) complex samples can bind to CT–DNA very strongly.

#### 3.3.2. Competitive DNA-binding studies with EB

In order to further investigate the interaction mode between the binuclear complexes and CT–DNA, the fluorescence titration experiments are performed. The fluorescence titration experiments, especially the EB fluorescence displacement experiment, have been widely used to characterize the interaction of complexes with DNA by following the changes in fluorescence intensity of the complexes. The intrinsic fluorescence intensities of DNA and that of EB in Tris–HCl buffer are low, while the fluorescence intensity of EB will be enhanced on addition of DNA as its intercalation into the DNA. Therefore, EB can be used to probe the interaction of complexes with DNA. If the complexes can intercalate into DNA, the binding sites of DNA available for EB will be decreased, and hence the fluorescence intensity of EB will be quenched [44]. In our experiments, as depicted in Fig. 3, for complex **1**, **2** and **3**, the fluorescence intensity of EB at 584 nm show a remarkable decreasing trend with the increasing concentration of the complex **1**, **2** or **3**,

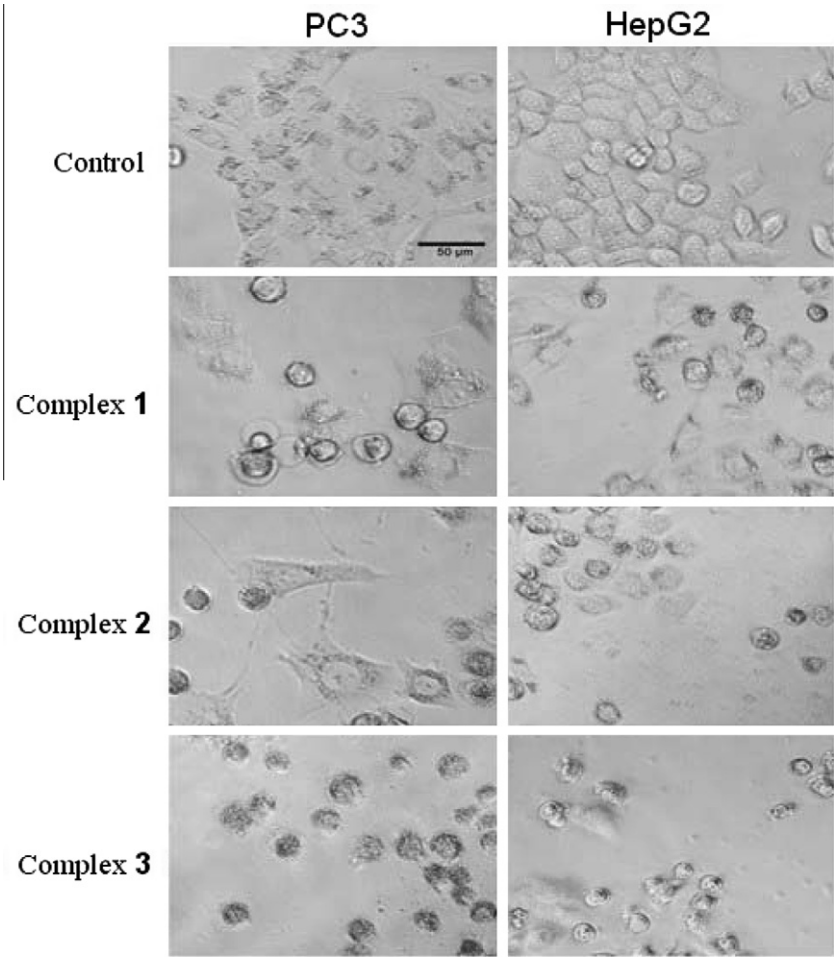


**Fig. 6.** Phase-contrast micrographs of cells treated with complexs **1**, **2** and **3**.

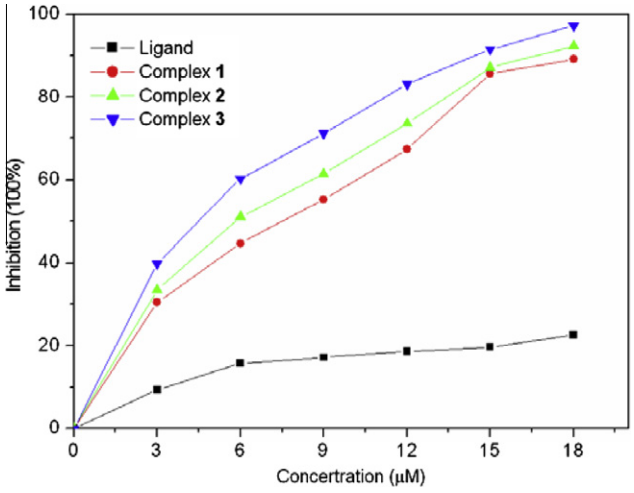


**Fig. 7.** Effect (%) of hydroxyl radical scavenging for ligand and Cu(II) complexes.

indicating that some EB molecules are released from EB–DNA after an exchange with the complex **1**, **2** or **3** which result in the fluorescence quenching of EB. This may be due either to the metal complex competing with EB for the DNA binding sites thus displacing the EB (whose fluorescence is enhanced upon DNA binding) or it should be a more direct quenching interaction on the DNA itself. We assume the reduction of the emission intensity of EB on increasing the complex concentration could be caused due to the displacement of the DNA bound EB by the ternary copper(II) complexes. The $K_q$ values of ternary copper(II) complexes are $2.81 \times 10^4\ M^{-1}$, $3.56 \times 10^4\ M^{-1}$, $6.16 \times 10^4\ M^{-1}$ for **1**, **2** and **3**, respectively. The order of $K_q$ for the complexes was very similar to the absorption titration methods and a similar explanation can be cited as stated earlier.

### 3.3.3. Circular dichroic spectral studies

Circular dichroic spectral techniques may give us useful information on how the conformation of the CT–DNA chain is influenced by the bound complex. The CD spectrum of CT–DNA consists of a positive band at 275 nm that can be due to base stacking and a negative band at 245 nm that can be due to helicity and it is also characteristic of DNA in a right-handed B form [45]. The changes in CD signals of DNA observed on interaction with drugs may often be assigned to the corresponding changes in DNA structure [46]. Thus simple groove binding and electrostatic interaction of small molecules show less or no perturbation on the base-stacking and helicity bands, whereas intercalation enhances the intensities of both the bands stabilizing the right-handed B conformation of CT–DNA as observed for the classical intercalator methylene blue [47,48].

The CD spectrum of CT–DNA is monitored in the presence of **1**, **2** and **3**, the changes observed in the three cases are shown in Fig. 4. On addition of all the complexes to CT–DNA, faint red shift with intensity increase in the positive or negative bands are observed. When addition of **3** to CT–DNA, it is observed that the

negative-band position was shifted to 246 nm with more evident increase than **1** and **2** in molar ellipticity, while the intensity of the positive band in the CD spectrum of DNA is perturbed remarkably with no shift. This phenomenon may be due to the intercalation of the complex through -stacking which stabilizes the right-handed B form DNA [49].

#### 3.3.4. Viscosity measurements

Optical photophysical probes provide necessary, but not sufficient clues to support a binding model. Hydrodynamic measurements (i.e., viscosity and sedimentation) that are sensitive to length change are regarded as the least ambiguous and the most critical tests of a binding model in solution in the absence of crystallographic structural data. A classical intercalation model results in lengthening the DNA helix as base pairs are separated to accommodate the bound ligand, leading to the increase of DNA viscosity. In contrast, a semi-intercalation of ligand could bend (or kink) the DNA helix, reduce its effective length, and concomitantly, its viscosity [50,51]. Fig. 5 depicts the effect of complexes **1**–**3** on the DNA viscosity. The change in relative viscosity for the dppz complexes are more than that for the phen or dpq analogues suggesting greater DNA binding propensity of the dppz complexes in comparison to the phen or bpq analogues. This is consistent with the observed trend shown by other optical methods and suggests primarily an intercalation binding nature of the complex.

### 3.4. Cytotoxic activity

To evaluate their cancer chemotherapeutic potential the ability of the DMSO soluble copper complexes **1**–**3** to kill human derived cancer cells was investigated using the human hepatic (HepG2), human promyelocytic leukemia (HL60) and human prostate (PC3) cell lines and was determined by calculation of $IC_{50}$ (the drug concentration causing a 50% reduction in cellular viability). Cells were continuously exposed to test agent for 72 h, and their effects on cellular viability was evaluated. It was intended that the results from these studies would allow the identification of those ternary derivatives with cancer chemotherapeutic potential. Comparison of $IC_{50}$ values, allowed the relative potency of each of the test compounds to be determined and ranked. The $IC_{50}$ values obtained for all tested compounds are presented in Table 4. The three metal complexes displayed a concentration-dependent cytotoxic profile in all cell lines. Since the $IC_{50}$ values for complexes **1**–**3** are statistically lower than that for metal-free heterocyclic bases and $H_2$PDIMAla in all of the tested cells, it suggests that coordinated copper(II) ion plays a major role in mediating potency of the complex. The $IC_{50}$ values for phen on all the cells are not statistically different, it displayed a greater effect against HL60 and HepG2 cell lines, which means phen is more sensitive than dpq and dppz for this two cell lines. All the heterocyclic bases show low $IC_{50}$ values against PC3 cell line. The results also suggest that **3** had more significant cytotoxic activities than **1** and **2** against the three human cancer cell lines, which is consistent with the result of DNA binding studies above. This may be due to the complexes inducing DNA damage in cancer cells and the nature of the compound itself.

In order to prove that the cytotoxicity observed is due to the ternary copper complexes, rather than to simple aquated metal ions $[Cu(H_2O)_x]^{y+}$, the ligand-free metal salts $Cu(ClO_4)_2{\cdot}6H_2O$, is screened against all the model cell lines. The data suggests that $Cu(ClO_4)_2{\cdot}6H_2O$ displayed significantly less effective than phen, $H_2$PDIAla and their metal complexes.

The morphology examinations also show that the proliferation of the cells are significant inhibited and the cells exhibit morphological changes such as cell shrinkage and cell detachment (Fig. 6).

### 3.5. Hydroxyl radical scavenging activity

Fig. 7 shows the plots of hydroxyl radical scavenging effect (%) for ligand and Cu(II) complexes, respectively, which are concentration-dependant. The values of $IC_{50}$ of ligand for hydroxyl radical scavenging effect cannot be read, while the values of $IC_{50}$ of Cu(II) complexes for hydroxyl radical scavenging effect are 4.5–7.5 μM with the order of **1 < 2 < 3**. These orders of $IC_{50}$ are opposite to the abilities of scavenging effects for hydroxyl radicals. It is marked that the hydroxyl radical scavenging effects of Cu(II) complexes are much higher than those of their ligand, possibly in that the larger conjugated metal complexes can react with $OH^{\cdot}$ to form larger stable macromolecular radicals than ligand [52]. Moreover, mannitol is a well-known natural antioxidant, so we also investigate the scavenging activity of mannitol against hydroxyl radical using the same model. We find that when arriving at similar suppression ratio, concentration of the two complexes is far less than that of mannitol.

## 4. Conclusions

A new reduced Schiff base ligand $H_2$PDIMAla and its three ternary copper(II) complexes are prepared and characterized, the DNA-binding properties of the complexes are investigated by absorption, fluorescence, circular dichroic spectral and viscosity measurements. The binding constant shows that the DNA-binding affinity increases in the order: complex **1** < complex **2** < complex **3**. Furthermore, the three copper(II) complexes have active scavenging effect on $OH^{\cdot}$. Although the mechanism between scavenging hydroxyl radicals should be also studied further, these findings clearly indicate that copper(II)-based complexes have many potential practical applications, like the development of nucleic acid molecular probes and new therapeutic reagents for diseases. On the other hand, the three complexes show considerable cytotoxic activity against three cell lines, and the $IC_{50}$ values of all the metal complexes are lower than that of phen and its substituted derivatives, $H_2$PDIMAla and $Cu(ClO_4)_2{\cdot}6H_2O$. Studies are currently underway in our laboratory to investigate more fully the mechanisms by which phen and its substituted derivatives, $H_2$PDIMAla and the three metal complexes control cancer cell viability. It is intended that the results from these studies will allow identification of key molecular targets, and in doing so will assist in elucidating their mechanisms of action, along with facilitating the development of highly effective anti-cancer therapies.

## Acknowledgment

We thank the Prof. Jagadese J. Vittal and Tan Geok Kheng for solving the crystal, the financial support of the Ministry of Education grant through National University of Singapore (Grant No. R143-000-371-112) and the National Natural Science Foundation of China (21001040).

## Appendix A. Supplementary material

CCDC 698877 contains the supplementary crystallographic data for this paper. These data can be obtained free of charge from The Cambridge Crystallographic Data Centre via www.ccdc.cam.ac.uk/data_request/cif. Supplementary data associated with this article can be found, in the online version, at http://dx.doi.org/10.1016/j.ica.2012.05.014.

## References

[1] B.B. Aggarwal, D. Danda, S. Gupta, P. Gehlot, Biochem. Pharmacol. 78 (2009) 1083.
[2] P.F. Neumann, M. Silverberg, Nature 213 (1967) 775.

[3] I. Sternlieb, C.J. Van den Hamer, S. Alpert, Nature 216 (1967) 824.
[4] J.R. Sorenson, J. Med. Chem. 19 (1976) 135.
[5] J.R. Sorenson, Prog. Med. Chem. 26 (1989) 437.
[6] D. Kovala-Demertzi, J. Inorg. Biochem. 79 (2000) 153.
[7] H.M. Butler, A. Hurse, E. Thursky, A. Shulman, Aust. J. Expt. Biol. Med. Sci. 47 (1969) 541.
[8] R.A. MacLeod, J. Biol. Chem. 197 (1952) 751.
[9] F.P. Dwyer, I.K. Reid, A. Shulman, G.M. Laycock, S. Dixon, Aust. J. Expt. Biol. Med. Sci. 47 (1969) 203.
[10] M. McCann, M. Geraghty, M. Devereux, D. O'Shea, J. Mason, L. O'Sullivan, Metal-Based Drugs 7 (2000) 185.
[11] B. Coyle, M. McCann, K. Kavanagh, M. Devereux, M. Geraghty, BioMetals 16 (2003) 321.
[12] S.Y. Tsang, S.C. Tam, L. Bremner, M.J. Burkitt, Biochem. J. 317 (1996) 13.
[13] H. Pervez, Z.H. Chohan, M. Ramzan, F.H. Nasim, K.M. Khan, J. Enzyme Inhib, Med. Chem. 24 (2009) 437.
[14] H. Pervez, N. Manzoor, M. Yaqub, A. Khan, K.M. Khan, F.H. Nasim, M.I. Choudhary, Lett. Drug Des. Discov. 7 (2010) 102.
[15] M.C. Linder, Mut. Res. 475 (2001) 141.
[16] C. Deegan, M. McCann, M. Devereux, B. Coyle, D.A. Egan, Cancer Lett. 247 (2007) 224.
[17] A.K. Patra, T. Bhowmick, S. Ramakumar, M. Nethaji, A.R. Chakravarty, Dalton Trans. (2008) 6966.
[18] R.K. Rao, A.K. Patra, P.R. Chetana, Polyhedron 27 (2008) 1343.
[19] J.D. Ranford, P.J. Salder, D.A. Tocher, J. Chem. Soc. Dalton Trans. (1993) 3393.
[20] A. Shulman, D.O. White, Chem. Biol. Interact. 6 (1973) 407.
[21] J.K. Barton, Science 233 (1986) 727.
[22] SMART and SAINT Software Reference Manuals, Versions 5.6 and 6.4, Bruker AXS, Madison, WI, 2003.
[23] G.M. Sheldrick, SADABS software for empirical absorption correction, University of Göttingen, Germany, 2003.
[24] SHELXTL Reference Manual, Version 6.14, Siemens Energy & Automation, Inc., Analytical Instrumentation, Madison, WI, 2003.
[25] A. Wolf, J.G.H. Shimer, T. Meehan, Biochemistry 26 (1987) 6392.
[26] M.R. Efink, C.A. Ghiron, Anal. Biochem. 114 (1981) 199.
[27] M. Eriksson, M. Leijon, C. Hiort, B. Norden, A. Gradslund, Biochemistry 33 (1984) 5031.
[28] Y. Xiong, X.F. He, X.H. Zou, J.Z. Wu, X.M. Chen, L.N. Ji, R.H. Li, J.Y. Zhou, K.B. Yu, Dalton Trans. (1999) 19.
[29] C.C. Winterbourn, Biochem. J. 182 (1979) 625.
[30] C.C. Winterbourn, Biochem. J. 198 (1981) 125.
[31] Z.Y. Guo, R.E. Xing, S. Liu, H.H. Yu, P.B. Wang, C.P. Li, P.C. Li, Bioorg. Med. Chem. Lett. 15 (2005) 4600.
[32] L. Yang, C.A. La, O.P. Anderson, D.C. Crans, Inorg. Chem. 41 (2002) 6322.
[33] M. Tsaramyrsi, M. Kaliva, A. Salifoglou, C.P. Raptopoulou, A. Terzis, V. Tangorlis, J. Giapintzakis, Inorg. Chem. 40 (2001) 5772.
[34] A.C. Rizzi, O.E. Piro, E.E. Castellano, O.R. Nascimento, C.D. Brondino, Inorg. Chim. Acta 305 (2000) 19.
[35] C.C. Su, Y.L. Lin, S.J. Liu, T.H. Chang, S.L. Wang, F.L. Liao, Polyhedron 12 (1993) 2687.
[36] A. Paulovicova, U. El-Ayaan, Y. Fukuda, Inorg. Chim. Acta 321 (2001) 56.
[37] C. Metcalfe, J.A. Thomas, Chem. Soc. Rev. 32 (2003) 215.
[38] M. Baldini, M. Belicchi-Ferrari, F. Bisceglie, P.P. Dall'Aglio, G. Pelosi, S. Pinelli, P. Tarasconi, Inorg. Chem. 43 (2004) 7170.
[39] B. Peng, H. Chao, B. Sun, H. Li, F. Gao, L.N. Li, J. Inorg. Biochem. 100 (2006) 1487.
[40] S.A. Tysoe, R.J. Morgan, A.D. Baker, T.C. Strekas, J. Phys. Chem. 97 (1993) 1707.
[41] A. Dimitrakopoulou, C. Dendrinou-Samara, A.A. Pantazaki, M. Alexiou, E. Nordlander, D.P. Kessissoglou, J. Inorg. Biochem. 102 (2008) 618.
[42] Q.G. Zhang, F. Zhang, W.G. Wang, X.L. Wang, J. Inorg. Biochem. 100 (2006) 1344.
[43] J.Z. Wu, L. Yuan, J.F. Wu, J. Inorg. Biochem. 99 (2005) 2211.
[44] R. Indumathy, S. Radhika, M. Kanthimathi, T. Weyhermuller, B.U. Nair, J. Inorg. Biochem. 101 (2007) 434.
[45] V.I. Ivanov, L.E. LMinchenkova, A.K. Schyolkina, A.I. Poletayer, Biopolymer 12 (1973) 89.
[46] P. Lincoln, E. Tuite, B. Norden, J. Am. Chem. Soc. 119 (1997) 1454.
[47] B. Norden, F. Tjerneld, Biopolymer 21 (1982) 1713.
[48] K. Kiridi, A. Garoufis, A. Tsipis, N. Hadjiliadis, H. Dulk, J. Reedijk, Dalton Trans. (2005) 1176.
[49] P.U. Maheswari, M. Palaniandavar, J. Inorg. Biochem. 98 (2004) 219.
[50] C.R. Brodie, J. Collins, J.R.A. Wright, Dalton Trans. (2004) 1145.
[51] C.S. Allardyce, P.J. Dyson, D.J. Ellis, S.L. Heath, Chem. Commun. (2001) 1396.
[52] J. Ueda, N. Saito, Y. Shimazu, T. Ozawa, Arch. Biochem. Biophys. 333 (1996) 377.